Unifying Decision Making and Trajectory Planning in Automated Driving through Time-Varying Potential Fields

Unifying Decision Making and Trajectory Planning in Automated Driving through Time-Varying Potential Fields ⋆

D. Costa * **F. Cerrito** * **M. Canale** * **C. Novara** *

* *Politecnico di Torino, Torino 10129, Italy.*

Abstract: This paper proposes a unified decision making and local trajectory planning framework based on Time-Varying Artificial Potential Fields (TVAPFs). The TVAPF explicitly models the predicted motion via bounded uncertainty of dynamic obstacles over the planning horizon, using information from perception and V2X sources when available. TVAPFs are embedded into a finite horizon optimal control problem that jointly selects the driving maneuver and computes a feasible, collision free trajectory. The effectiveness and real-time suitability of the approach are demonstrated through a simulation test in a multi-actor scenario with real road topology, highlighting the advantages of the unified TVAPF-based formulation.

Keywords: Trajectory and path planning for AVs, Autonomous vehicles, Control architectures in automotive control.

1. INTRODUCTION

Advanced Driver Assistance Systems (ADAS), such as Anti-lock Braking Systems (ABS), Electronic Stability Programs (ESP), and automatic emergency braking, have significantly improved road safety. Autonomous Vehicles (AVs) aim to extend these benefits to transportation efficiency and accessibility, but they require reliable onboard, real-time Trajectory Planning (TP) that respects traffic laws, passenger comfort, vehicle dynamics limitations, and interactions with uncertain external actors.

A key limitation of many AV architectures is the separation between high-level decision making (DM) and low-level TP. Hierarchical solutions based on supervisory logic or behavior switching mechanisms, e.g., Zheng et al. (2024); Wang et al. (2024), work well in structured settings but become less robust in multi-actor scenarios, where several events may overlap and conflicting objectives must be handled jointly. Likewise, decoupled approaches that plan path and speed separately, e.g., Yang et al. (2024), may produce decisions that are locally reasonable yet dynamically infeasible or overly risky in the future. For this reason, integrating DM and TP within a single framework is highly desirable (Liu et al., 2025; Fu et al., 2025).

Artificial Potential Fields (APFs), originally introduced by Khatib (1986), are widely used for real-time obstacle avoidance: repulsive fields encode obstacles, while attractive fields guide the vehicle toward the target. However, standard APFs rely on *static* environment representations and are mainly used in gradient-based planners (Zhu et al., 2006; Rostami et al., 2019), they do not explicitly capture the predicted evolution and uncertainty of surrounding actors. In road scenarios, such uncertainty arises from incomplete V2X information, sensor fusion errors, or the absence of intent communication. Adaptive APF variants partly address this issue by exploiting additional vehicle data (Lin and Tsukada, 2022; Lu et al., 2020), but they still do not directly guarantee safety with respect to future actors' behavior.

To address these challenges, this work proposes a *Time-Varying* Artificial Potential Field (TVAPF) formulation for unified decision making and trajectory planning. The APF evolves over the Local Trajectory Planner (LTP) prediction horizon using the available perception and V2X information, so dynamic obstacles are modeled together with their uncertainty. By embedding the TVAPF in a Finite Horizon Optimal Control Problem (FHOCP), the system simultaneously selects the driving maneuver and computes a physically feasible trajectory, resulting in coherent real-time actions. The main contributions of this paper are summarized as follows:

(1) A novel TVAPF formulation that explicitly accounts for the predicted evolution and uncertainty of dynamic obstacles.
(2) A tailored FHOCP that unifies DM and TP while generating physically feasible trajectories.
(3) Validation in a challenging multi-actor scenario with real road topology, showing the effectiveness and real-time viability of the proposed framework.

Notation The set of integers over a specific interval $[0, a]$ is denoted as: $\mathbb{N}_a = \{i \in \mathbb{N} \mid 0 \leq i \leq a\}$. FHOCP objective functions are denoted by a boldface letter $\mathbf{F}_{\mathrm{obj}}$. The standard FHOCP notation is used to denote predictions. The predicted value x at time instant $k + j$, computed using information available at the current time instant k, is denoted by $x(k+j|k)$. The weighted P-norm of a vector x for $P \succeq 0$ is defined as $\|x\|_P = \sqrt{x^\top P x}$.

2. PROBLEM SET-UP

This section introduces the coordinate reference frames used in the proposed approach. Then, the comprehensive AV control architecture is presented, detailing its subsystems and their functional interconnections.

2.1 Reference Frames

As illustrated in Fig. 1, the framework uses two frames. The first is a global Cartesian frame defined by the (X, Y) axes. This represents a natural choice for describing the external environment and allows direct definitions of Euclidean distances and absolute road geometries. In contrast, to effectively define and manage geometric constraints related to road boundaries, curvature, and lane positioning, the LTP problem is formulated using a local Frenet frame. In this frame, the state of a generic AV is described by the longitudinal coordinate s (representing the curvilinear distance along the path) and the lateral

⋆ This publication is part of the project Piano Nazionale di Ripresa e Resilienza (PNRR)- Next Generation Europe, which has received funding from the Italian Ministry of University and Research – DM 117/2023

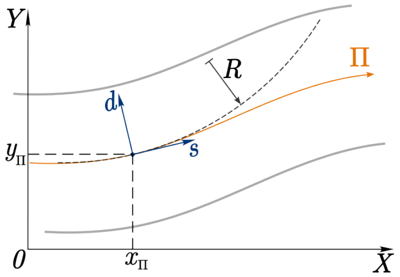

Fig. 1. Architecture reference frames. —Cartesian coordinates, —Frenet-Serret coordinates, —GPP reference path Π, and —Road boundaries.

offset d (representing the perpendicular distance from the path).

Remark 1. For a regular $\mathcal{C}^2$ path curve, a bijective analytic map $\mathcal{T}_{\mathrm{cf}}$ transforms Cartesian coordinates to Frenet coordinates with a well-defined inverse (see $\mathcal{T}_{\mathrm{fc}}$ Zheng et al. (2020)).

2.2 Control architecture

Although the focus of this work is on designing a LTP, its definition is critically dependent on a systematic and complete view of the full control architecture. This structure is pivotal for properly identifying how information is collected and processed across different functionalities, thereby ensuring a well-posed control problem. Thus, this section describes the control architecture (Fig. 2), providing details on the implementation and information flow.

- The *Global Path Planner* (GPP) computes the route to the destination based on a priori and infrastructure information, generating a reference geometric path characterized by edges and lane curvature information. Road attributes, such as the number of lanes and speed limitations, are also provided to generate safe trajectories. The path is derived via standard methods, e.g., vision-based detection for highways, or graph-search algorithms like A^* or Dijkstra (cf. (Cheng et al., 2014; Hart et al., 1968)) combined with geometric smoothing (Dubins, clothoids, cf. (Canale and Razza, 2024)) for unstructured areas. A detailed description of the GPP is omitted, however, the geometric properties of its output are critical:

  Definition 1. The reference path Π is a $\mathcal{C}^2$ curve represented by a sequence of Cartesian samples $[x_\Pi, y_\Pi]^\top$ (see Fig. 1), satisfying Remark 1.
- The *APF* block operates as an intermediate layer between the external environment (including GPP information, V2X communication, and vehicle sensor data) and the LTP. The main goal of this block is to obtain a unified description of the environment, capable of handling a multi-objective problem: maximizing passenger comfort, ensuring obstacle avoidance, guaranteeing compliance with traffic rules, and respecting vehicle dynamics. To this purpose, TVAPF enables the external actors' uncertain motion to be accounted for within the subsequent LTP block.
- The *LTP* processes inputs, including the reference path characteristics from the GPP, APF information, and the current ego-vehicle state χ. The planning task is formulated as a function of the APFs information within a FHOCP. The solution to this FHOCP, solved with a suitable instance period, yields the optimal state trajectory Ξ^* over the prediction horizon T_L, which the ego-vehicle tracks to execute safe, collision-free maneuvers while satisfying performance objectives.
- The *Trajectory Resampling and Synchronization* block receives as input the optimal trajectory Ξ^* computed by the LTP. By exploiting the coordinate transformation $\mathcal{T}_{\mathrm{fc}}$ and employing a linear resampling technique to account for potential mismatches between the Ξ^* discretization and the motion controller sampling time, it generates a suitable reference state trajectory χ_{ref} required for the tracking control layer.
- A *Motion Controller* (MC) computes the final low-level control actions, such as steering and acceleration, required to track the resampled optimal trajectory χ_{ref} computed by the LTP. Many well-known solutions (Calzolari et al., 2017) can be exploited for this purpose.

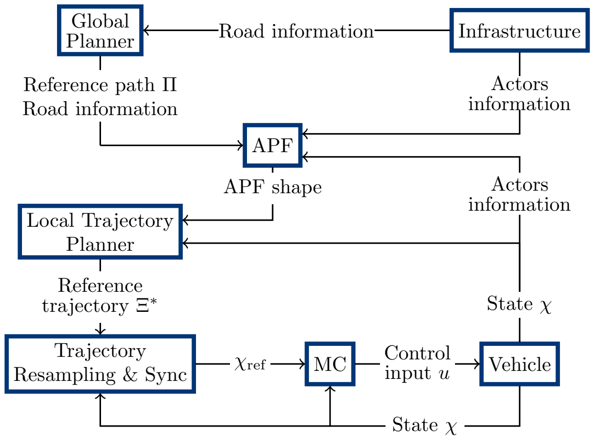

Fig. 2. Control structure architecture and exchanged information.

It is worth noting that, in the proposed architecture, the necessity of making a priori discrete decisions based solely on the current state of the system is eliminated. The core of the approach, the APF block, operates as a container for a unified mathematical description of both the actual state and the predicted uncertain states of the environment. Many scenarios (e.g., V2V, V2I, or absence of communication) can be handled within the same general scheme.

3. TRAJECTORY PLANNER OBJECTIVES

This section introduces the speed tracking objective and static APFs, then presents the proposed TVAPF formulation, including its safety guarantees and how it uses available information to improve trajectory planning.

3.1 Speed Tracking Objective

One of the primary objectives of the LTP is to track a desired longitudinal velocity profile. To this end, the planner targets a desired vehicle speed v_{des}, which is upper-bounded by the maximum allowed speed on the road segment $v_{\max}$. Furthermore, for passenger comfort, the vehicle lateral acceleration must be bounded by a threshold $a_{l,\max}$. While the constraint can be statically mapped to the road curvature, dynamic maneuvers such as lane changes require a consideration of the instantaneous angular rate of the trajectory, denoted as ω. To ensure the lateral acceleration constraint $a_y \approx v^2|\omega| < a_{l,\max}$ is satisfied, the vehicle speed must be dynamically limited. To address all these requirements, an effective reference speed $\bar{v}$ is introduced. This variable represents the most restrictive constraint among the desired speed, the regulatory speed limit, and the dynamic comfort limit derived from the instantaneous angular rate. The effective reference speed is mathematically defined as:

$$\bar{v} = \min\left\{ v_{\mathrm{des}}, v_{\max}, \sqrt{\frac{a_{l,\max}}{|\omega|}} \right\}. \tag{1}$$

A quadratic cost $\mathbf{W}_v$ is utilized to penalize deviations from this effective reference:

$$\mathbf{W}_v(v,\bar{v}) = (v-\bar{v})^2 \,. \tag{2}$$

This formulation ensures that the vehicle tracks the desired speed when it is possible, but seamlessly yields to comfort and safety constraints.

3.2 Static APFs

To ensure that the vehicle remains strictly within the road boundaries, repulsive APFs characterized by a Gaussian profile are established along the left (l) and right (r) road edges. Given a generic boundary i and its Euclidean distance from the vehicle h_i, the potential field $\mathbf{W}_b^i(h_i)$ is defined as:

$$\mathbf{W}_b^i(h_i) = e^{-(\eta h_i)^4}, \;\; i = l, r \,. \tag{3}$$

The coefficient $\eta > 1$ is used to tune the smoothness of the repulsive potential's transition. The full road boundary APF $\mathbf{W}_b(h)$ is then obtained by the superposition of the left and right boundary APFs:

$$\mathbf{W}_b(h) = \mathbf{W}_b^l(h_l) + \mathbf{W}_b^r(h_r) \,. \tag{4}$$

The formulation ensures that the vehicle remains within road boundaries; however, it does not by itself ensure compliance with standard road regulations, which require keeping the rightmost free lane. To address this, an additional APF $\mathbf{W}_l(h_c)$ is introduced. This term generates a virtual attractive force that guides the vehicle toward the preferred lane position. The APF is defined as a function of h_c, the minimum distance between the ego vehicle and the left boundary of the rightmost free lane.

$$\mathbf{W}_l(h_c) = \frac{1}{(1+e^{h_c})} \,. \tag{5}$$

To ensure lane centering, as detailed in related works (Canale et al., 2024), it is not necessary to introduce a new APF. Rather, proper parameter computation can be achieved by imposing suitable analytical conditions on the existing APFs.

3.3 Time-Varying APF

The LTP must be able to handle dynamic obstacles with uncertain future states. In fact, without V2X communication, the ego vehicle relies on on-board sensors and requires conservative predictions that cover the actors' reachable states. With V2X, richer intent information is available, but uncertainty remains due to communication latency and model prediction errors in the received data. The prediction uncertainty associated with surrounding actors is formalized through the uncertain prediction vector Δ_i (6). For a generic obstacle i at a future time step $k+j$, predicted based on information available at the current time k, this vector is defined as:

$$\Delta_i(k+j|k) = [\delta s_i(k+j|k) \;\; s_{o,i}(k+j|k)]^\top \,. \tag{6}$$

This vector encapsulates two fundamental parameters: the estimated longitudinal uncertainty spread δs, and the predicted central longitudinal position of the obstacle s_o. Given this characterization, the TVAPF is defined to penalize collision risks dynamically over the prediction horizon:

$$\mathbf{W}_o(k+j|k) = e^{-\left(\left(\frac{s-s_o(k+j|k)}{\gamma_s(k+j|k)}\right)^c + \left(\frac{d-d_o(k)}{\gamma_d}\right)^c\right)}, \quad c \in \mathbb{N}^+_{\text{even}} \,.$$

$$\gamma_s(k+j|k) = \frac{\delta s(k+j|k)+\sigma_s}{\alpha_s}, \quad \gamma_d = \frac{l_W+\sigma_d}{\alpha_d} \,. \tag{7}$$

In this formulation, $\mathbf{W}_o$ represents the potential field magnitude at the predicted instant $k+j$. The parameters σ_s and σ_d denote the tunable safety margins that the ego vehicle is required to maintain longitudinally and laterally, respectively. The exponent c governs the sharpness of the potential function's gradients, while l_W defines the lateral occupancy of the obstacle field and is selected equal to the lane width. Finally, α_s and α_d are scaling factors which, following the methodology applied to lane APFs, are computed to ensure that specific boundary conditions are satisfied at the limits of the safety zone.

In the following, the specific definition of TVAPF parameters is detailed in a scenario characterized by the absence of V2X communication. We emphasize that this condition, while representing the most challenging operational scenario for the LTP, constitutes also the necessary fallback procedure in the event of V2X subsystem faults.

Given the initial obstacle state at time k, defined by longitudinal position $s_o(k)$, lateral position $d_o(k)$, and speed $v_o(k)$, the TVAPF parameters are computed for each step j of the prediction horizon. The state evolution is propagated using the following discrete-time prediction model:

$$\begin{cases} s_o(k+1) = s_o(k) + T_{s,L} v_o(k) \\ v_o(k+1) = v_o(k) + T_{s,L} a_o(k) \end{cases} \tag{8}$$

where $T_{s,L}$ denotes the sampling time of the LTP and a_o the obstacle acceleration. Due to physical limitations of vehicle actors, speed and acceleration are limited within the bounds $[v_{o,\min}, v_{o,\max}]$ and $[a_{o,\min}, a_{o,\max}]$, respectively. Consequently, the maximum and minimum reachable longitudinal positions, denoted as $s_{o,\max}(k+j|k)$ and $s_{o,\min}(k+j|k)$, are calculated for each prediction step by propagating these bounding dynamics and applying saturation constraints throughout the horizon.

To populate the vector introduced in (6), the longitudinal uncertainty spread δs is defined as the spread of the reachable set at prediction step $k+j$:

$$\delta s(k+j|k) = |s_{o,\max}(k+j|k) - s_{o,\min}(k+j|k)| \tag{9}$$

Similarly, the center of the uncertainty area is defined as the geometric center of the reachable set:

$$s_o(k+j|k) = \frac{s_{o,\max}(k+j|k) + s_{o,\min}(k+j|k)}{2} \tag{10}$$

***Remark** 2.* The uncertain area defined by equations (9) and (10), and the consequent TVAPF formulated in (7), constitute a *compact bounded set* within the Frenet frame. This property is mathematically guaranteed by the inherent definition of the uncertainties, which are derived from physical constraints. Furthermore, due to the bounded dynamics governing vehicle motion described in (8), the time evolution and prediction of the potential field $\mathbf{W}_o$ are guaranteed to remain bounded over the entire prediction horizon.

4. OPTIMAL CONTROL PROBLEM FOR TRAJECTORY PLANNING

In this section, we first define the prediction model utilized within the FHOCP. Subsequently, the FHOCP formulation designed to unify DM and TP is detailed, and its key features are discussed.

4.1 Prediction model

Since the aim of the FHOCP is the generation of a feasible vehicle trajectory, the material point model reported in (11) is utilized to account for the time behavior of the ego-vehicle:

$$\begin{cases} \dot{s}(t) = \nu(t)\cos(\psi(t)) \\ \dot{d}(t) = \nu(t)\sin(\psi(t)) \\ \dot{\psi}(t) = \omega(t) \\ \dot{\nu}(t) = \alpha(t) \end{cases} \tag{11}$$

where s and d represent the vehicle's longitudinal and lateral positions in the Frenet frame, respectively. The variable ψ denotes the heading angle, ν represents the longitudinal speed, while α and ω correspond to the longitudinal acceleration and heading rate control inputs, respectively. To derive the discrete-time model required for the FHOCP predictions, the state vector is defined as $\xi =$

$[s, d, \psi, \nu]^\top$ and the control input vector as $\lambda = [\alpha, \omega]^\top$. The prediction model (12) is then obtained by discretizing the continuous dynamics (11) using the zero-order hold method with a sampling time of $T_{s,L}$.

$$\xi(k+1) = f(\xi(k), \lambda(k)) \tag{12}$$

4.2 Optimal Control Problem

The LTP problem is cast as an FHOCP defined as a function of the uncertainties collected in the parameter matrix Δ, the system control input sequence Λ, and the consequent predicted plant state Ξ.
The matrices collecting the necessary information over the prediction horizon N_L are defined as follows:

(1) Uncertainties Matrix $\Delta(k)$: collects the predicted uncertainties for all n_o obstacles. It is defined as the matrix formed by the vectors $\Delta_i(k+j|k)$, where the row index $i \in \mathbb{N}_{n_o}$ corresponds to the obstacle and the column index $j \in \mathbb{N}_{N_L}$ corresponds to the prediction step.
(2) Control Input Sequence $\Lambda(k)$: the vector containing the sequence of optimized control inputs, defined as $\Lambda(k) = [\lambda(k|k)^\top, \ldots, \lambda(k+N_L-1|k)^\top]^\top$.
(3) Predicted State Sequence $\Xi(k)$: the vector containing the predicted state evolution, defined as $\Xi(k) = [\xi(k+1|k)^\top, \ldots, \xi(k+N_L|k)^\top]^\top$.

The cost function (13) used in the FHOCP is composed of different objectives that penalize undesirable states or control actions, each multiplied by a proper weighting factor. The objectives previously described (e.g., function of speed, distances) can now be explicitly defined as functions of the optimization variables and parameters (Λ, Ξ, Δ). The FHOCP objective terms included in (13) are:

- $\mathbf{W}_v(\Xi)$: with cost weight K_v, this term penalizes deviations from the desired speed profile.
- $\mathbf{W}_b(\Xi)$: with cost weight K_b, this term enforces the vehicle to stay within lane boundaries.
- $\mathbf{W}_l(\Xi)$: with cost weight K_l, this term guides the vehicle toward the rightmost free lane.
- $\mathbf{W}_c(\Xi, \Lambda)$: with cost weight K_c, this term ensures proper passenger comfort by penalizing high lateral acceleration.

Finally, the term $\mathbf{O}(\Delta, \Xi)$ encompasses the contribution of the TVAPFs, which are crucial to account for the prediction uncertainties of surrounding actors. As defined in (7), this term encapsulates the influence of all uncertainties related to the surrounding vehicles, integrating available information from various sources (e.g., V2X, sensors). Following Remark 2, the total uncertainty area defined by $\mathbf{O}$ is a finite sum of compact bounded sets, ensuring that $\mathbf{O}$ itself is compact and bounded.
For brevity, the detailed dependence on Λ, Ξ, and Δ will be implied in the formulation of the total cost function $\mathcal{J}$. The complete cost function $\mathcal{J}$ to be minimized is defined over the prediction horizon N_L as:

$$\mathcal{J}(\Lambda, \Xi, \Delta) = \sum_{j=0}^{N_L} (K_v \mathbf{W}_v + K_b \mathbf{W}_b + K_l \mathbf{W}_l + K_c \mathbf{W}_c + K_o \mathbf{O}) \,, \tag{13}$$

$$\mathbf{O}(j) = \sum_{i=1}^{n_o} \mathbf{W}_{o,i}(\Delta_i(k+j|k)) \,. \tag{14}$$

The optimal vehicle trajectory is defined as the computed optimal state sequence Ξ^* that minimizes the cost function (13). Although the proposed optimization setup may appear similar to standard MPC formulations, the primary goal in the proposed approach is different. The objective is not to evaluate the optimal control action $\lambda(k|k)$ at the current time instant, but to determine the entire state prediction Ξ^* over the horizon N_L, which defines the optimal trajectory to be tracked by the MC. The trajectory Ξ^* is finally the direct output of LTP.

$$\Xi^* = \underset{\Lambda(k), \Xi(k)}{\arg\min}\ \mathcal{J}(\Lambda, \Xi, \Delta) \tag{15}$$

subject to :

$$\begin{aligned}
&\xi(k|k) = \xi(k) \\
&\xi(k+j+1|k) = f(\xi(k+j|k), \lambda(k+j|k))\,, && \forall j \in \mathbb{N}_{N_L-1}\,, \\
&\xi(k+j|k) \in \mathcal{A}_\xi\,, && \forall j \in \mathbb{N}_{N_L}\,, \\
&\lambda(k+j|k) \in \mathcal{A}_\lambda\,, && \forall j \in \mathbb{N}_{N_L-1}\,, \\
&\Delta\lambda(k+j|k) \in \mathcal{A}_{\Delta_\lambda}\,, && \forall j \in \mathbb{N}_{N_L-2}\,, \\
&\mathbf{O}(\Delta, j) \leq \varepsilon_o\,, && \forall j \in \mathbb{N}_{N_L}\,, \\
&\xi(k+N_L|k) \in \mathcal{A}_{\xi,f}\,.
\end{aligned}$$

To ensure trajectory feasibility, different constraints are introduced on the system dynamics and operational limits. Firstly, the plant state evolution is constrained by the actual vehicle state and must strictly adhere to the discrete prediction model (12) over the entire horizon. To ensure compliance with both actuator feasibility limits and passenger comfort requirements, admissible sets are formally defined for the system variables. Specifically, we introduce $\mathcal{A}_\xi$ for the state vector, $\mathcal{A}_\lambda$ for the control inputs, and $\mathcal{A}_{\Delta_\lambda}$ for their respective rates of variation. Finally, to guarantee safety, the vehicle's predicted position is constrained by the obstacle uncertainty TVAPF. This constraint ensures that the vehicle never crosses a region that could potentially be occupied by other actors over the prediction horizon. Consequently, the obtained optimal trajectory Ξ^* is safe despite the uncertain behavior of the surrounding actors. Although recursive feasibility is not the central concern of this work, it can be enforced by defining a terminal safe-stop set. The terminal state is thus constrained to a region from which a collision-free braking maneuver is guaranteed to exist. A more detailed explanation and a sketch of the proof of recursive feasibility under such a safe-stop terminal construction can be found in Costa et al. (2026).

Example 1. Fig. 3 illustrates the effectiveness of the TVAPF in unifying DM and TP within a highway scenario involving a leading vehicle (A) and an approaching vehicle on the left lane (B). The snapshots depict the TVAPF evolution over the prediction horizon for a single LTP instance. In the top scenario, the LTP successfully computes an overtaking maneuver, as evidenced by the ego vehicle avoiding the uncertain regions of the TVAPF. Conversely, in the bottom scenario, the proximity of vehicle B renders the overtake unsafe; consequently, the LTP concurrently *decides* to keep the current lane and *plans* a coherent lane-keeping trajectory to maintain a safe distance. Although this example highlights a single time step, the FHOCP is solved iteratively at runtime to continuously adapt to environmental state updates and uncertainties.

Remark 3. (Motion Controller) An NMPC scheme is used as MC to track the LTP reference trajectory. A complete description of the NMPC MC implementation is available in Costa et al. (2026).

5. SIMULATION RESULTS

The simulation test is developed via MATLAB and Simulink tools. The *Roadrunner* environment is used to define the driving scenario, and the *Vehicle Dynamics Blockset* is employed to simulate vehicle dynamics. In this setup, only the actual state of the surrounding vehicles in the ego vehicle sensor range is known. The relevant optimization problems involved in the LTP and the NMPC

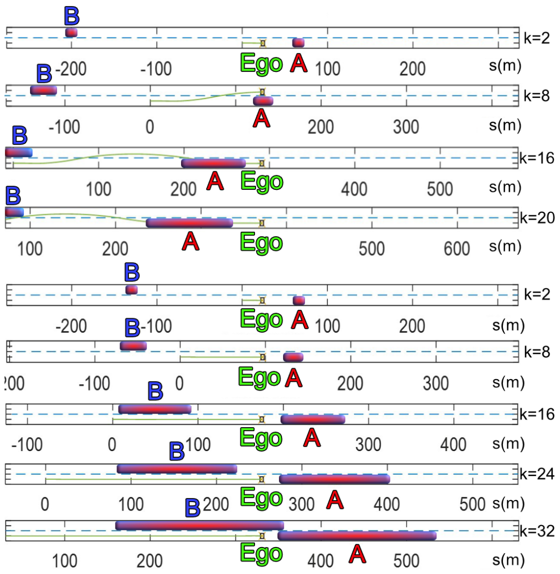

Fig. 3. TVAPF prediction in the LTP FHOCP. Top: Feasible overtaking maneuver. Bottom: The LTP detects collision risk, deciding to maintain the current lane behind vehicle A.

Table 1. LTP and NMPC FHOCP parameters

Parameter	LTP	NMPC
Sample time T_s	0.5 s	0.2 s
Prediction horizon	35 s	2 s
Instance period	5 s	0.2 s

Fig. 4. Overview of the scenario in Roadrunner, detailing the position of the ego vehicle and the actors (L1,O1,O2) before the overtake maneuver.

Table 2. Vehicles kinematic limits

Parameter	Unit	Minimum	Maximum
Speed v	m/s	0	12.5
Longitudinal acceleration a	m/s^2	-0.9	0.9
Jerk $\dot{a}$	m/s^3	-0.9	0.9
Yaw rate $\dot{\theta}$	deg/s	-4.44	4.44
Steering angle δ	deg	-24.5	24.5

are solved with the *Ipopt* solver using CasADi as a development framework. The parameters used for the OCPs are reported in Table 1. In all simulations performed, the maximum LTP optimization time was 0.23 s while the mean was 0.031 s on an Intel i5-1340P CPU.

For the simulation test [1], we consider the driving scene represented in Fig. 4 consisting of a suburban two-way road with lane width $l_W = 4$ m and maximum speed limitation of 12.5 m/s. In this scene, besides the ego vehicle, three actors are present: L1 traveling ahead of the ego in the same direction and, in the other lane, the actors O1, O2 moving in the opposite direction. All vehicles are considered subject to the constraints in Table 2.

The scenario starts with the ego vehicle entering a 1.5 km road segment at an initial speed of 8.33 m/s, with a reference velocity of 12 m/s. The lead vehicle L1 is located 300 m ahead, traveling at a lower speed of 3 m/s (see Fig. 4) and, in this condition, an overtaking maneuver has to be performed by the ego vehicle. The scenario is characterized by the dynamic behavior of the surrounding actors. In fact, as the ego vehicle closes the gap to L1, the oncoming vehicle O1 approaches (Fig. 4) and accelerates with $a_{\max}$ from 6 m/s to 10 m/s. Simultaneously, the lead vehicle L1 accelerates up to 6 m/s. Furthermore, the second oncoming vehicle O2, located behind O1, approaches at a constant speed of 8 m/s. Under these dynamic conditions, the LTP must adapt the vehicle speed to ensure collision avoidance. Concurrently, it must determine the optimal timing and trajectory for a physically feasible and comfortable overtaking. In particular, the simulation starts with the ego vehicle accelerating to reach the reference speed of 12 m/s (Fig. 6 A). At 15 s, the LTP receives information about the position and velocity of L1 and O1, and TVAPFs are computed to predict their worst-case behavior. Thus, in the next two LTP instances (at 20 s and 25 s), the LTP decides to delay the overtake maneuver as all overtake trajectories are rendered infeasible by the TVAPF. Consequently, the LTP progressively reduces the ego speed to 8.6 m/s to keep a safe distance from L1. Furthermore, Fig. 6 A shows that the deceleration speed profile directly results from the sequence of LTP instances, rather than from a static velocity target. In the next LTP instance, at 30 s, even the worst-case prediction encoded by the TVAPF allows the ego to perform the overtake maneuver, and an initial overtaking path is computed.

In the successive LTP instances at 35 s, 40 s, and 45 s, the feasible overtaking path is progressively refined (Fig. 5), accounting for the arrival of another oncoming vehicle in the left lane (O2) and by the usage of new information that reduces the uncertainty in the predicted positions of O1 and L1. Finally, at 55 s, the ego has completed the maneuver and returned to the rightmost lane with no leading vehicle, thus it seamlessly resumes tracking the lane center at the reference speed (Fig. 6).

In summary, despite the uncertain dynamics of the surrounding actors, the proposed architecture effectively manages the timing of the overtaking maneuver. Furthermore, it ensures the generation of a safe trajectory that is continuously reshaped as a function of the most accurate information available at each planning instance. During the entire simulation, passenger comfort is also preserved, as illustrated by the g–g diagram in Fig. 6 B, where both longitudinal and lateral accelerations remain within the imposed limits.

6. CONCLUSION

This paper presents a unified framework for the DM-TP of AVs, exploiting a novel TVAPF formulation. By modeling the future state evolution and bounded uncertainties of dynamic obstacles, the proposed method seamlessly integrates information from both on-board perception and V2X information. The embedding of these dynamic fields within a tailored FHOCP enables the simultaneous evaluation of the most suitable driving maneuver and the consequent generation of a physically feasible trajectory. Simulation results in a dynamic multi-actor scenario characterized by real road topology demonstrated the effectiveness of the approach. The framework successfully generates strategically coherent behaviors while satisfying safety and comfort constraints. Future work will focus on extending the architecture to more complex scenarios, with particular emphasis on intersection handling.

REFERENCES

Calzolari, D., Schürmann, B., and Althoff, M. (2017). Comparison of trajectory tracking controllers for autonomous vehicles. In *2017 IEEE 20th Interna-*

[1] Animation video of the simulation: `https://youtube.com/playlist?list=PLaJBGNRMGh8KrlUwjy9TqowIFCURIfwDC&si=oSGsbinLMCf03ize`.

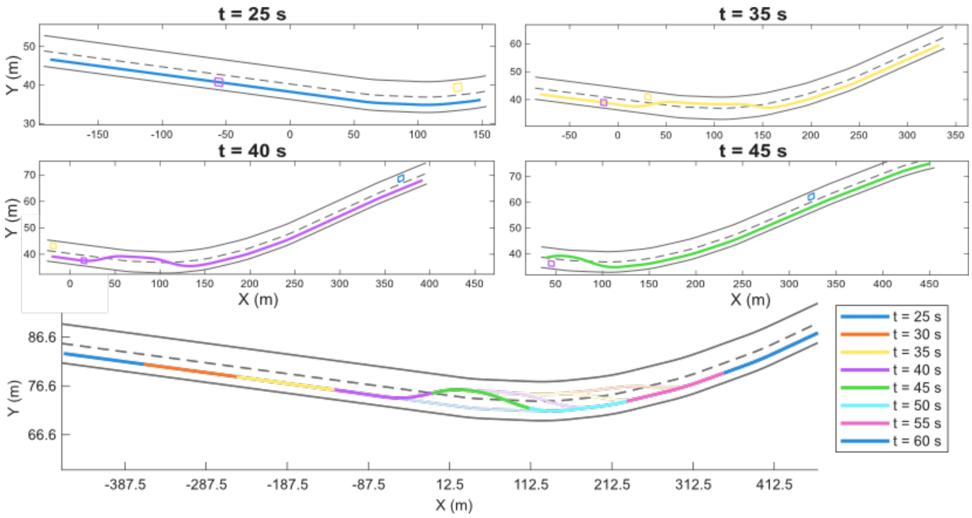

Fig. 5. LTP trajectories: Top: Predicted trajectory at a specific LTP instance, showing the current position of the actors. Bottom: Trajectory segments followed by the ego vehicle, including semi-transparent extensions that represent the complete predicted path at each LTP instance.

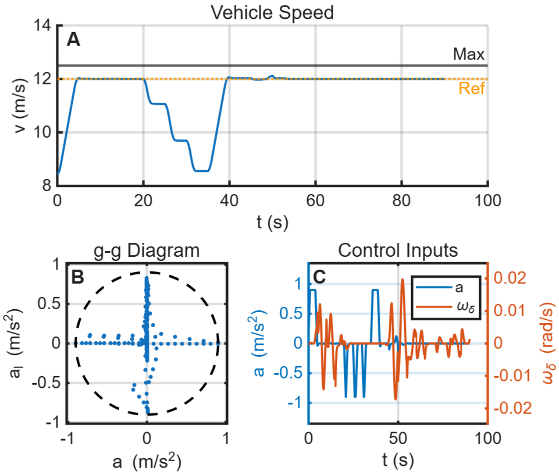

Fig. 6. Simulation results: A - Vehicle speed. B - g-g diagram. C - Control Inputs.

tional Conference on Intelligent Transportation Systems (ITSC), 1–8.

Canale, M., Cerrito, F., and Borodani, P. (2024). An ego-based approach to planning and control for automated valet parking applications. In *2024 IEEE 63rd Conference on Decision and Control (CDC)*, 8193–8198.

Canale, M. and Razza, V. (2024). Automated driving control in highway scenarios through a two-level hierarchical architecture. *IEEE Access*, 12, 86470–86486.

Cheng, L., Liu, C., and Yan, B. (2014). Improved hierarchical A-star algorithm for optimal parking path planning of the large parking lot. In *2014 IEEE International Conference on Information and Automation (ICIA)*, 695–698.

Costa, D., Cerrito, F., Canale, M., and Novara, C. (2026). Unifying decision making and trajectory planning in automated driving through time-varying potential fields. URL `https://arxiv.org/abs/2603.13136`.

Fu, T., Zhou, H., and Liu, Z. (2025). Integrated decision-making and path planning framework for autonomous driving in multi-lane obstacle avoidance. *Proceedings of the Institution of Mechanical Engineers, Part D: Journal of Automobile Engineering*, 15.

Hart, P.E., Nilsson, N.J., and Raphael, B. (1968). A formal basis for the heuristic determination of minimum cost paths. *IEEE Transactions on Systems Science and Cybernetics*, 4(2), 100–107.

Khatib, O. (1986). Real-time obstacle avoidance for manipulators and mobile robots. *The International Journal of Robotics Research*, 5(1), 90–98.

Lin, P. and Tsukada, M. (2022). Adaptive potential field with collision avoidance for connected autonomous vehicles. In *2022 13th Asian Control Conference (ASCC)*, 2251–2256.

Liu, W., Liu, H., Zheng, L., Huang, Z., and Ma, J. (2025). Synergizing decision making and trajectory planning using two-stage optimization for autonomous vehicles. *IEEE Transactions on Vehicular Technology*, 74(4), 5489–5503.

Lu, B., Li, G., Yu, H., Wang, H., Guo, J., Cao, D., and He, H. (2020). Adaptive potential field-based path planning for complex autonomous driving scenarios. *IEEE Access*, 8, 225294–225305.

Rostami, S.M.H., Sangaiah, A.K., Wang, J., and Liu, X. (2019). Obstacle avoidance of mobile robots using modified artificial potential field algorithm. *EURASIP Journal on Wireless Communications and Networking*, 2019(1), 70.

Wang, X.F., Chen, W.H., Jiang, J., and Yan, Y. (2024). High-level decision-making for autonomous overtaking: An mpc-based switching control approach. *IET Intelligent Transport Systems*, 18(7), 1259–1271.

Yang, H., He, Y., Xu, Y., and Zhao, H. (2024). Collision avoidance for autonomous vehicles based on mpc with adaptive apf. *IEEE Transactions on Intelligent Vehicles*, 9(1), 1559–1570.

Zheng, L., Zeng, P., Yang, W., Li, Y., and Zhan, Z. (2020). Bézier curve-based trajectory planning for autonomous vehicles with collision avoidance. *IET Intelligent Transport Systems*, 14(13), 1882–1891.

Zheng, X., Li, H., Zhang, Q., Liu, Y., Chen, X., Liu, H., Luo, T., Gao, J., and Xia, L. (2024). Intelligent decision-making method for vehicles in emergency conditions based on artificial potential fields and finite state machines. *Journal of Intelligent and Connected Vehicles*, 7(1), 19–29.

Zhu, Q., Yan, Y., and Xing, Z. (2006). Robot path planning based on artificial potential field approach with simulated annealing. In *Sixth International Conference on Intelligent Systems Design and Applications*, volume 2, 622–627.